SOCAR Proceedings

Drilling & Completion

journal home page: http://proceedings.socar.az

DESIGNING COMBINATIONS OF TECHNICAL AND TECHNOLOGICAL FACTORS THAT ENSURE THE EFFICIENCY OF DRILLING OPERATIONS AT GREAT DEPTHS

R. A. Hasanov, J. R. Gasimova

Azerbaijan State Oil and Industry University, Baku, Azerbaijan

A B S T R A C T

Study of rock failure under excessive pressure drawdown is associated with the lack of an effective flushing system design. In this process, the filtration rate of drilling fluid through the bottomhole plays a key role. The pressure drawdown effect is fully realized when the rate of penetration exceeds the fluid filtration rate in both destruction and pre-destruction zones. If the penetration rate is equal to or lower than the filtration rate, the effect becomes only partial. The efficiency of a drill bit largely depends on the performance of its hydraulic system. The main criterion is the ability to promptly remove drilled cuttings from the bottomhole zone. To achieve effective cleaning, the flushing system must direct the drilling fluid, after reflecting from the bottomhole surface, toward the central channel of the bit. Such a flow pattern – from the periphery to the center – ensures efficient removal of accumulated cuttings. Various drill bit designs are currently used in well construction, making it important to evaluate their effectiveness under comparable rock destruction conditions. The primary performance indicator is the rate of penetration, defined as the volume of rock drilled per unit time. Deep well drilling practice shows that significant energy losses occur during transmission to the bottomhole due to depth. Under such conditions, abrasive-cutting tools are the most effective, providing high penetration rates with minimal energy consumption. Additionally, penetration per single impact is a critical parameter for selecting optimal drilling modes and ensuring maximum efficiency. This approach improves drilling performance, reliability, and overall operational stability.

Keywords: wells, mechanical model, centrifugal force, drilling, ball velocity, fluid viscosity, washing channel, graphical solution.

Date submitted: 19.11.2025 **Date accepted:** 20.02.2026 **Date published:** 20.05.2026

Introduction

The efficiency of any bottomhole assembly with a bit, regardless of its design features, as many researchers note, is largely determined by the performance of the flushing system [1-6]. Its level of perfection is characterized by the ability to timely clean the bottomhole zone from drilled cuttings during the drilling process [7-10]. Such efficiency can only be achieved by meeting the requirements imposed on the design of the bit flushing system [11]. The key requirement is that the flushing fluid entering the bottomhole must, after impinging on the rock surface, be directed into the central channel of the tool. Only with such flow movement (from the periphery of the bottomhole to its center) are conditions created for effective removal of sludge accumulating at the bottomhole during drilling operations [2, 3, 12].

To study the characteristics of flushing fluid movement, its interaction with the well bottomhole is represented as a mechanical model shown in figure 1 [7, 11, 13, 14].

The mathematical description of the interaction process between the drilling fluid and the bottomhole is formulated in the XOY coordinate system, the origin of which is located at the nozzle exit from the nozzle, on its axis. It is assumed that the drilling fluid, conditionally represented as spherical particles with radius r_0 (r_0 corresponds to the radius of the nozzle outlet), leaves the nozzle with velocity v_0 at an angle α to the vertical y-axis destruction parameters.

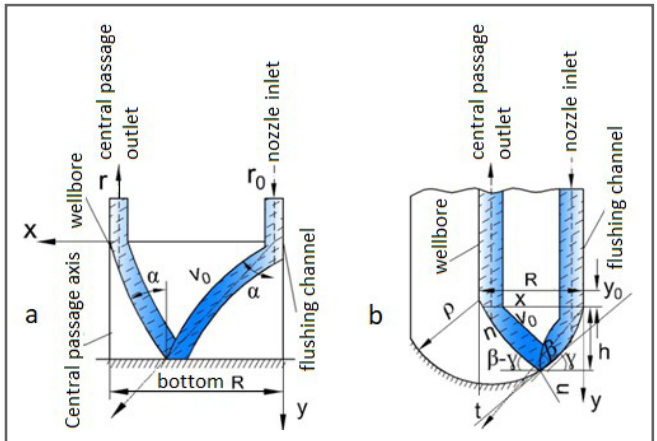

Fig. 1. Mechanical model of drilling fluid interaction with the bottomhole of flat (a) and spherical (b) wellbore shapes:
h – nozzle height; α – angle between the jet direction and y-axis; β – reflection angle of the drilling fluid jet; R – distance between the nozzle axis and the central passage axis; r – radius of the device central channel

***E-mail:** ramiz.hasanov52@gmail.com

http://dx.doi.org/10.5510/OGP2026SI101171

On a spherical body placed isn a stationary fluid, both medium resistance and centrifugal force act simultaneously. The action of the fluid on the sphere can be described through a complex coefficient ξ, taking into account its movement velocity υ and the medium viscosity μ.

The centrifugal force is directed opposite to the x-axis and is expressed by the formula

$$F = m\omega^2(R-x)$$

where m is defined as the object's mass considered particle; ω is the angular velocity of bit rotation; x is defined as the distance from the rotation center to the ball at a given moment.

Thus, the motion of the ball as a material point can be described by a system of equations in projections onto the coordinate axes [13, 15].

$$\begin{aligned} &m\ddot{x} + 6\pi\mu r_0\dot{x} + m\omega^2(R-r) = 0; \\ &m\ddot{y} + 6\pi\mu\dot{y} = 0. \end{aligned} \tag{1}$$

where x and y are the coordinates of the ball center at time t; the dot above the quantities x and y denotes the time derivative.

Substituting into expression (1), we obtain:

$$\begin{aligned} &\ddot{x} + \frac{9\mu}{2\rho_f r_0^2}\dot{x} - \omega^2 R = -\omega^2 R; \\ &\ddot{y} + \frac{9\mu}{2\rho_f r_0^2}\dot{y} = 0. \end{aligned} \tag{2}$$

The solution of equation (2) will be:

$$x = C_1 e^{K_1 t} + C_2 e^{K_2 t} + R, \tag{3}$$

where C_1, C_2 are integration constants; K_1, K_2 are parameters whose values are determined as follows:

$$\left.\begin{aligned} K_1 &= -K - \sqrt{K^2+\omega^2} = -K - m \\ K_2 &= -K + \sqrt{K^2+\omega^2} = -K + m \end{aligned}\right\},$$

here

$$K = \frac{9\mu}{4\rho_f r_0^2}; \quad m = \sqrt{K^2+\omega^2}$$

Considering that $x(0) = 0$; at $t = 0$ the integration constants C_1 and C_2 are determined as:

$$C_1 = \frac{\upsilon_0 \sin\alpha + RK_2}{K_1 - K_2}; \quad C_2 = \frac{\upsilon_0 \sin\alpha + RK_1}{K_2 - K_1}.$$

Substituting the values of coefficients K_1 and K_2 into the formula for determining C_1 and C_2

$$x = e^{-kt}(C_1 e^{-mt} + C_2 e^{mt}) + R. \tag{4}$$

Then equation (2) takes the form:

$$y = C_3 e^{-2kt} + C_4. \tag{5}$$

The constants C_3 and C_4 are determined from the boundary condition $y(0) = 0$; at $t = 0$, and take the form $C_3 = \frac{-\upsilon_0 \cos\alpha}{2K}$; $C_4 = \frac{\upsilon_0 \cos\alpha}{2K}$, which allow the following expression to be obtained for the vertical coordinate y.

$$y = \frac{\upsilon_0 \cos\alpha}{2K}(1 - e^{-2kt}). \tag{6}$$

From equation (6), we determine the time t_0 at which the ball reaches the bottom of the well under the boundary condition $t = t_0$ at $y = h$:

$$t_0 = \frac{1}{2K}\ln\frac{\upsilon_0 \cos\alpha}{\upsilon_0 \cos\alpha - 2hK}. \tag{7}$$

The upward motion of the ball is described by equations similar to (2) and has the following solution:

$$\begin{aligned} x_1 &= C_5 e^{k_2 t} + C_6 e^{k_2 t} + R; \\ y_1 &= C_7 e^{-2kt} + C_8 \end{aligned} \tag{8}$$

Knowing the boundary conditions:

$$\left.\begin{aligned} &X_1(0) = X(t_o); \quad \dot{X}_1(0) = \upsilon(t_o)\cos\beta = \dot{X}(t_o) \\ &y_1(0) = h; \qquad \dot{y}_o(0) = \upsilon(t_o)\sin\beta = -\dot{y}(t_0) \end{aligned}\right\} \quad \text{at } t = 0.$$

The constants C_5, C_6, C_7 and C_8 can be determined from the following equations:

$$\begin{aligned} C_5 &= \frac{\dot{X}(t_o) - K_2\left[X(t_o) - R\right]}{K_1 - K_2}; \quad C_7 = \frac{\dot{y}(t_o)}{2K}; \\ C_6 &= \frac{\dot{X}(t_o) - K_1\left[X(t_o) - R\right]}{K_2 - K_1}; \quad C_8 = h - \frac{\dot{y}(t_o)}{2K}. \end{aligned} \tag{9}$$

According to the design requirements for the flushing system, after the drilling fluid impinges on the bottomhole, it must be directed into the central passage to ensure the suction effect. This condition must be satisfied at height h after the fluid reflects off the bottomhole. Mathematically, it is expressed as $x_1 = R$ at $y_1 = 0$, which is accounted for in the following equation:

$$\frac{R(m-K) + \upsilon_o \sin\alpha}{R(m+K) - \upsilon_o \sin\alpha} = \left(\frac{\upsilon_o \cos\alpha - 2hK}{4hK - \upsilon_o \sin\alpha}\right)^{\frac{m}{k}} \tag{10}$$

The angle α, which determines the jet direction, as well as the installation height and nozzle diameter, are incorporated in expression (10). In addition, the drilling fluid flow rate Q is included in the formula through υ_0. Given values for any three of the four parameters, the remaining one may be calculated from equation (10), which enables theestablishment of a centrifugal jet flow pattern. Thus, equation (10) serves as a mathematical algorithm for selecting the design characteristics of flushing systems for rock cutting tools with central supply, ensuring effective cleaning of the bottomhole zone from drilled cuttings. Additionally, the condition $\upsilon(t) \geq 0$ must be satisfied, that is:

Similarly, the situation when the bottomhole has a spherical shape (fig. 1b) can be considered. It is assumed that the center of the sphere is located on the well axis, so its coordinates are given as point $O_1(R, y_0)$, where y_0 is a specified value. The circular cross-section in this case is described by the equation:

$$\left(X - R\right)^2 + \left(y - y_o\right)^2 = \rho^2 \tag{11}$$

where ρ is the sphere radius.

According to (10), the equation of motion for the drilling fluid passing through the nozzles can be determined as follows:

$$X = \sqrt{\frac{\upsilon_o \cos\alpha - 2Ky}{\upsilon_o \cos\alpha}}\left[\begin{aligned} &C_1\left(\frac{\upsilon_o \cos\alpha - 2Ky}{\upsilon_o \cos\alpha}\right)^{\frac{m}{2k}} + \\ &+C_2\left(\frac{\upsilon_o \cos\alpha - 2Ky}{\upsilon_o \cos\alpha}\right)^{\frac{m}{2k}} \end{aligned}\right]. \tag{12}$$

The motion of the drilling fluid flowing out of the nozzles is described by the formula given in expression (10):

$$y = \frac{R - X(t_o)}{y(t_o) - y_o} \cdot X + \frac{RX(t_o) - y_o(t_o) - R^2 - y_o^2 + \rho^2}{y(t_o) - y_o} \qquad (13)$$

It can be seen from Figure 1b that the jet is reflected at angles β and γ, the values of which can be determined from the formulas:

$$\cos\beta = \frac{\dot{X}(t_o)}{\sqrt{\dot{X}^2(t_o) + \dot{y}^2(t_o)}}; \qquad tg\gamma = \frac{R - X(t_o)}{y(t_o) - y_o} \qquad (14)$$

In (8), the integration constants C_5, C_6, C_7, C_8 can be determined from the following boundary conditions:
here

$$\upsilon(t_o) = \sqrt{\dot{X}^2(t_o) + \dot{y}^2(t_o)}.$$

From (10), taking into account the boundary conditions, C_5, C_6, C_7, C_8 can be determined as:

$$C_5 = \frac{\upsilon(t_o)\cos(\beta - \gamma) + K_2\left[R - X(t_o)\right]}{K_1 - K_2};$$

$$C_6 = \frac{\upsilon(t_o)\cos(\beta - \gamma) + K_1\left[R - X(t_o)\right]}{K_2 - K_1};$$

$$C_7 = \frac{\upsilon(t_o)\sin(\beta - \gamma)}{2K}; \quad C_8 = y(t_o) - \frac{\upsilon(t_o)\sin(\beta - \gamma)}{2K}.$$

The time for the drilling fluid to reach the spherical bottomhole can be deter-mined from the boundary condition $y_1 = 0$ at $x_1 = R$:

$$t_1 = -\frac{1}{2K}\ln\left(-\frac{C_8}{C_7}\right) = \frac{1}{K}\ln\sqrt{\frac{\upsilon(t_o)\sin(\beta - \gamma)}{\upsilon(t_o)\sin(\beta - \gamma) - 2Ky(t_o)}} \qquad (15)$$

Taking into account (13) and (8), we obtain the relationship between the design parameters of the rock-cutting tool flushing system and the drilling operation modes:

$$C_5 + C_6\left[\frac{\upsilon_o \sin(\beta - \gamma)}{\upsilon_o \sin(\beta - \gamma) - 2Ky(t_o)}\right]^{\frac{m}{k}} = 0 \qquad (16)$$

In addition to the parameters contained in the transcendental equation (10), equation (16) includes the angle γ, which is determined by the sphere curvature radius ρ. Consequently, expression (16) is more general compared to (10), since the latter represents a particular case obtained at $\rho \to \infty$. Thus, formula (16) serves as a mathematical basis for designing both the structure of the flushing system of rock-cutting tools with central feed and the corresponding operating parameters, including the design of the executive body, i.e., the cutting structure of the tool.

The mechanical models of the interaction process (fig. 1a and b) confirm the feasibility of this approach, on the basis of which Eqs. (10) and (16) were derived [3, 4, 8, 11]. Comparison of the schemes in figure 1 shows that with a spherical bottomhole shape having a center shifted upward, easier suction of drilling cuttings in the bottomhole zone is ensured. This corresponds to the design of the executive body with a concave central cutting part. In the opposite case, when the sphere center is located below the bottomhole, i.e., the executive body has a convex cutting surface, cuttings removal becomes more complicated. Consequently, the optimal shape of the tool cutting part lies in the region of concave designs, while the least effective is the flat-bottom shape of the cutting part.

Figure 2 presents curves demonstrating the influence of operating factors and various combinations of flushing system design parameters [16].

As shown in the graphs, as the nozzle distance from the bottomhole increases, the initial velocity of the flushing fluid jet rises sharply. At the same time, maximum growth is observed at a nozzle inclination angle to the vertical of approximately 30°, which corresponds to the interval $15° \le \alpha \le 45°$. Beyond this range, changes in the initial jet velocity become relatively insignificant.

2. Evaluation of energy consumption in rock destruction and development of optimal design parameters for flushing nozzles of rock-cutting tool flushing systems

In modern drilling practice, bits of various structural designs are used. The¬re-fore, an urgent task is to determine the efficiency of rock-cutting tools applied under real conditions and operating at identical rock destruction parameters [4, 17].

As the main indicator of destruction effectiveness, the specific energy consumption of the process is usually considered, i.e., the volume of rock removed per unit time [11, 13, 15]. Experience in deep well drilling shows that with significant increase in depth and the associated difficulties in energy transfer to the bottomhole, abrasive-cutting type rock-cutting tools become most effective [7, 5]. They ensure maximum penetration per single bit run with minimum energy expenditure. It should be emphasized that the magnitude of penetration per bit run is of great importance when selecting rational drilling modes ensuring high trip speed.

A key direction for improving drilling efficiency and economic outcomes, especially in deep wells, is the more rational application of the hydraulic power of the directed

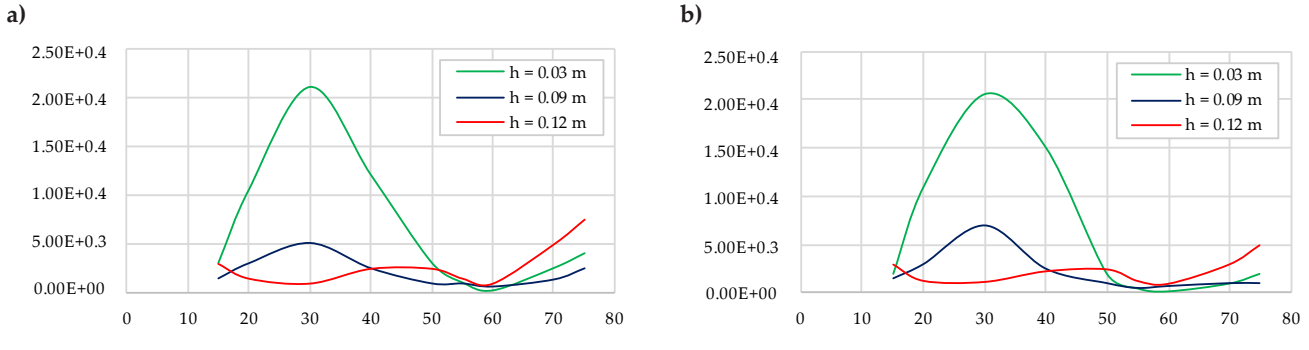

Fig. 2. Dependence of drilling modes on the flushing system design: a) r = 0.012 m, r_o = 0.009 m; b) r = 0.04 m, r_o = 0.009 m

fluid flow [6]. Research on different types of jet bits, performed under laboratory and field conditions worldwide, has shown that nozzles with elliptical inlets and sharper outlets yield the greatest discharge coefficients (up to 0.99) [8-10]. As a consequence, extra hydraulic power becomes available and may be directed toward increasing the penetration rate. Hence, choosing the optimal geometry and profile of jet bit nozzle channels is essential for improving drilling efficiency.

Defining these parameters from the condition of maximum submerged jet flow impact allows the resistance at jet discharge from the nozzles to be minimized. Knowing the optimal outlet diameter, one can further determine the rational internal channel profile, as well as select the most suitable inlet section diameter.

Solution of these problems by traditional methods proves difficult, since when selecting the initial nozzle diameter, data on flow resistance forces are absent. In such a situation, classical approaches of optimal control prove especially effective [11, 18, 19]. The formulated problem of determining flushing channel parameters is as follows.

It is necessary to determine the optimal function on the interval , ensuring uniform velocity distribution along the nozzle length with minimum hydraulic power losses. For its solution, the equation of fluid motion in the nozzle is written in the following form:

$$m\frac{dv}{dt} = p(t)F(t), \qquad p(t) = \frac{Q^2\gamma}{2g\omega^2F^2(t)}, \tag{17}$$

where m is the mass of fluid flowing inside the nozzle; υ is the jet flow velocity at the current point of the nozzle; is the current cross-sectional area of the nozzle channel; is the circulating fluid flow rate; is the specific weight of the flushing fluid; is the discharge coefficient.

In accordance with the optimality criterion, the following system of equations is formed:

$$\frac{dx_1}{dt} = \frac{1}{m}p(t)F(t) = f_1, \qquad \frac{dx_0}{dt} = k_1x_2^1 + k_2F^2(t) = f_\circ \tag{18}$$

Then for the conjugate variables, we obtain the following formula:

$$\frac{d\psi_1}{dt} = \sum_{i=1}^{n}\frac{\partial f_i}{dx_i}\psi_1, \qquad \psi_\circ = -1, \qquad \frac{d\psi_1}{dt} = -2k_1x_1\psi_0. \tag{19}$$

According to the optimization method, the Hamiltonian is formulated as:

$$H = \sum_{i=1}^{n}\psi_i f_i;$$

or, writing the expression in expanded form:

$$H = -\left(k_1x^2 + k_2F_{(t)}^2\right) + \psi_1\frac{Q^2\gamma}{2gm\omega^2}F(t).$$

From the above formula, let us extract the terms containing:

$$H^* = -k_2F^2(t) + \psi_1\frac{Q^2\gamma}{2gm\omega^2}F(t), \tag{20}$$

Hence:

$$-k_2F^2(t) + \psi_1\frac{Q^2\gamma}{2gm\omega^2}\cdot F(t) =$$
$$= -k_2\left(F_t - \frac{Q^2\gamma\psi_1}{4gm\omega^2k_2}\right)^2 - \frac{Q^4\gamma^2\psi_1^2}{16g^2m^2\omega^2k_2^2}.$$

Substituting $F(t) = Q^2\gamma / 4gm\omega^2k_2$ into formula (18), we obtain:

$$\frac{dx_1}{dt} = \frac{1}{2k_2}\left(\frac{Q^2\gamma}{2gm\omega^2}\right)^2\psi_1; \qquad \frac{d\psi_1}{dt} = 2k_1x(t). \tag{21}$$

The boundary conditions allowing the solution of equation (21) to be determined are given below:

$$\upsilon(t=0) = \upsilon_0; \quad F(t=0) = F_0$$
$$\upsilon(t=T) = \upsilon_{out}; \quad F(t=T) = F_{out}$$

Then the solution of equation (21) is:

$$F(t) = \frac{F_0F_{out}shBT}{F_{out}shBTchBt + F_0shBT - F_{out}shBtchBT}$$

$$\upsilon(t) = \upsilon_0(chBt - chBTshBt) + \frac{shBT}{shBT}\upsilon_{out} \tag{22}$$

Using the theorem on the change of fluid momentum along the nozzle length, we obtain:

$$\frac{Q\gamma t}{g}(\upsilon(t) - \upsilon_{out}) = \frac{\upsilon_{(t)}^2 - \upsilon_{out}^2}{2g\omega^2}\cdot tF(t). \tag{23}$$

At the same time, it is obvious that $\upsilon(t) = \upsilon_{out}$, $F(t) = F_{out} = F_0$ at $t = 0$.

Solving equation (23) with respect to F_0, we obtain the following relationship for the sought quantity:

$$F_0 = \frac{(2\omega^2Q - \upsilon_{out}F_{out})}{\upsilon_{out}} \tag{24}$$

Equation (22), taking into account Eq. (24), takes the following form

$$F(t) = \frac{(2\omega^2Q - \upsilon_{out}F_{out})F_{out}shBT}{2\omega^2QshBt + \upsilon_{out}F_{out}[shB(T-t)] - shBt'} \tag{25}$$

and

$$\upsilon(t) = (chBt - shBtchBt)\frac{\upsilon_{out}F_{out}}{F_0} + \upsilon_{out}\frac{shBT}{shBT}. \tag{26}$$

Formula (25) represents the expression for the longitudinal section profile of the nozzle. From (26), the velocity variation in any nozzle section can be determined:

$$\upsilon(t) = \frac{1}{B}(chBt - chBtchBt)\frac{\upsilon_{out}F_{out}}{F_0} + \frac{1}{B}\upsilon_{out}\frac{chBT}{shBT}. \tag{26a}$$

The nozzle length l can be determined when $y(t = T) = l$.

Thus, to determine the nozzle length, the following relationship must be used:

$$l = \left(shBT - \frac{ch^2BT}{shBT}\right)\frac{\upsilon_{out}F_{out}}{F_0} + \frac{\upsilon_{out}chBT}{BshBt} + \\ + \frac{\upsilon_{out}F_{out}}{BF_0}chBT - \frac{\upsilon_{out}}{BshBt} \tag{27}$$

Using formulas (25) and (26), calculations can be performed for specific cases ($Q = 0.04$ m³/hour; $F_{exit} = 6.4 \cdot 10^{-3}$ m²; $B = 198$ sek⁻¹; $\upsilon_{exit} = 70$ m/sek) (figs. 3, 4).

Thus, the determined optimal nozzle profile shapes allow substantially reducing local hydraulic resistances and ensuring the maximum possible discharge coefficient value $\omega = 1$ [5, 6, 8-10]. This is confirmed by the data presented in figure 4: the flow velocity in each nozzle section varies uniformly and increases along its length, which is consistent with the results of foreign experimental studies.

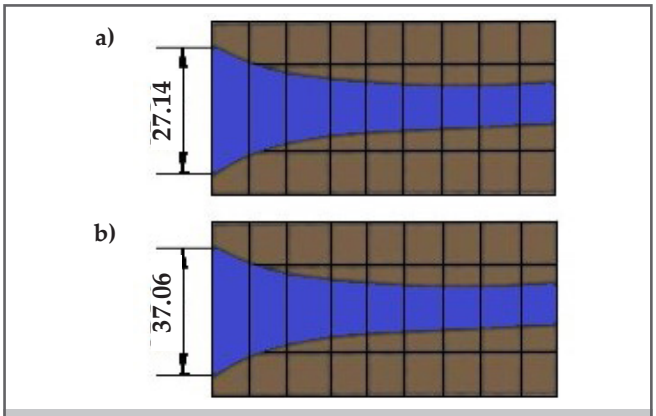

Fig. 3. Nozzle profile at a discharge coefficient of 0.75 (a) and 1 (b)

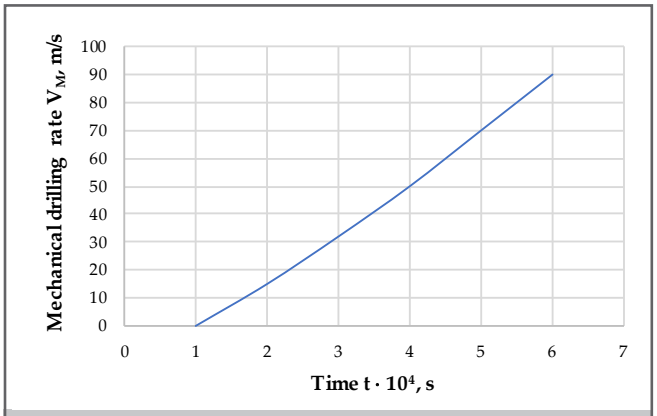

Fig. 4. Dependence of rate of penetration on time for various nozzle profiles

3. Influence of excess dynamic pressure differential on rock destruction efficiency

During drilling, the drilling fluid or its filtrate delivered to the bottomhole must overcome the resistance of cuttings accumulated in the bottomhole zone [2, 4, 16, 20]. Depending on the direction and regime of fluid injection, forces may be generated that suppress rock breakage. The influence of these suppressive forces at the bottomhole can be significantly reduced by adjusting the properties of the drilling mud, optimizing drilling parameters, and designing rock-cutting tools with a specialized flushing system [1, 19, 21].

Analysis of rock fragmentation under conditions of high pressure differential, resulting from the lack of an effective design calculation method for bit flushing systems, does not always lead to the expected drilling efficiency.

In commercially produced bits, the drilling fluid is delivered to the bottomhole either in a vertical direction or at a specified angle. In such cases, the jet issuing from the bit flushing channels impacts the bottomhole and changes its direction, leading not only to a loss of kinetic energy but also to a significant reduction in the rotational component of the submerged jet. This component is particularly important under conditions of suppressive pressure differential, as it is required to generate jet-induced torque on the bottomhole surface.

During rock failure under an excessive pressure drop, the velocity of fluid flow through the bottomhole zone is of significant importance [13, 22, 23]. The influence of the pressure differential becomes fully effective only when the penetration speed of the cutting tool is consistently higher than the filtration velocity of the fluid within the fractured and near-fracture zones. When the tool penetration rate is equal to or lower than the fluid filtration rate, the action of the pressure differential is realized only to a limited extent.

For this reason, it becomes necessary to formulate the task of evaluating the values of inhibiting forces and torques that arise under conditions of an excessive pressure differential.

Since viscoplastic fluid is used as the flushing agent during well drilling, the flow exiting the bit nozzle to lift particles from the destruction zone must overcome the ultimate shear stress force or the corresponding resistance moment, i.e.:

$$\left.\begin{aligned} R_1 &= \tau_{\text{dyn}} \cdot F_1 = F_1\left(\tau_0 + \eta\frac{dv}{dr}\right); \\ M_1 &= R_1 \cdot r_{\text{aver.}} = F_1\left(\tau_0 + \eta\frac{dv}{dr}\right) r_{\text{aver}}. \end{aligned}\right\} \quad (28)$$

Here, F_1 denotes the bottomhole area exposed to the action of the flushing fluid; τ_{dyn} represents the dynamic shear stress; τ_0 is the limiting shear stress; η is the dynamic viscosity coefficient; dv/dr characterizes the velocity gradient near the bottomhole surface; raver is the mean radius of friction. For the bottomhole zone, it may be accepted approximately that $\tau_{aver} = D_c / 3$, where D_c is the diameter of the wellbore.

When an excessive pressure differential exists in the rock failure zone, the resulting resisting force or resisting torque must be compensated for by the liquid streams discharged from the flushing channels of the drill bit.

$$\left.\begin{aligned} R_2 &= F_2 \cdot \Delta P \\ M_2 &= F_2 \cdot \Delta P \cdot r_{\text{aver}} \end{aligned}\right\} \quad (29)$$

In this expression, F_2 denotes the filtration area of the well bottomhole, while ΔP characterizes the additional pressure difference acting within the rock failure and pre-failure zones.

It should be emphasized that, prior to the onset of rock destruction, the bottomhole is subjected to a static pressure differential. However, once the destruction process begins, this pressure difference acquires a dynamic nature.

Consequently, the overall inhibiting force, or the total moment generated by these inhibiting forces, can be calculated using the following relationship:

$$\left.\begin{aligned} R &= F_1\tau_{\text{dyn}} + F_2 \cdot \Delta P \\ M &= \left(F_1\tau_{\text{dyn}} + F_2 \cdot \Delta P\right) \cdot r_{\text{aver}} \end{aligned}\right\} \quad (30)$$

At the outlet cross-section, the velocity of the fluid particle is denoted by v_2, and this velocity forms an angle α_2 with the tangent to the trajectory. The radial distances from the centers of the inlet and outlet cross-sections to the rotational axis are represented by r_1 and r_2, respectively, as shown in figure 5.

The variation in the angular momentum of the fluid passing through the flushing orifices, considered with respect to the axis of rotation of the well, may then be determined as follows:

$$\frac{dL_z}{dt} = M_Z^E \quad (31)$$

Assume that at a given instant t, the fluid volume denoted as "abcd" is located inside one of the flushing channels of the drill bit. After a short time interval, at $t + \Delta t$, this same fluid volume shifts to the position "a1b1c1d1" During the time interval dt, the elementary volume of fluid entering the channel is equal to the elementary volume leaving it. Therefore, the mass of fluid passing through one flushing

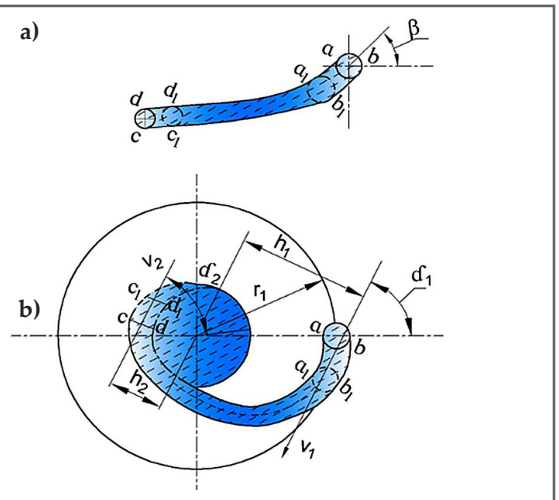

Fig. 5. Diagram of the drill bit flushing channel system: the projections of the flushing channel path onto the vertical plane (a) and the horizontal plane (b), respectively

channel during the time dt may be written as:

$$m_1 = m_2 = m\frac{\gamma Q}{N_g}dt = \frac{\rho Q}{N}dt \tag{32}$$

where ρ is the drilling mud density; Q is the pump flow rate; N is the number of flushing channels.

The change in the principal angular momentum of volume "abcd" about the z-axis during time dt is determined, considering the bit rotation direction as positive. This change equals the difference between the angular momenta of volumes "dcc_1d_1" and "abb_1a_1":

$$dL_{\text{chan.}} = mv_2h_2 - mv_1h_1 \tag{33}$$

where h_1 and h_2 are the moment arms of vectors and from the axis of rotation, respectively, determined by the formula:

$$\left.\begin{aligned} h_1 &= r_1 \cdot \cos\alpha \\ h_2 &= r_2 \cdot \cos\alpha \end{aligned}\right\} \tag{34}$$

where r_1 and r_2 are the distances from the axis of rotation to the centers of the inlet and outlet of the flushing channels, respectively.

Substituting (32), (33), (34) into (31), we obtain:

$$M_Z^E = \frac{dL_Z}{dt} = \rho Q\,(v_2r_2\cos\alpha_2 - v_1r_1\cos\alpha_1) \tag{35}$$

The change in angular momentum of all flushing channels during time t equals:

$$dL_Z = [\rho Q\,(v_2r_2\cos\alpha_2 - v_1r_1\cos\alpha_1)]\,dt \tag{36}$$

The pressure exerted by the fluid on the walls of the flushing channel is balanced by wall reaction forces of the same magnitude but acting in the opposite direction. As a result, the fluid produces a rotational moment Mrot on the drill bit, which is numerically equal to this moment but has the opposite sign. Therefore, it can be expressed as follows:

$$M_{rot} = -M_Z^E = -\rho Q\left(v_1r_1\cos\alpha_1 - v_2r_2\cos\alpha_2\right) \tag{37}$$

Accordingly, the torque generated by the fluid discharged from the flushing channel depends directly on the fluid density, the flow rate, and the difference between the products of the velocity components and their corresponding shortest distances to the axis of rotation. In order to increase the torque produced by the fluid leaving the bit channel, the outlet section of the flushing channel should be arranged as close as possible to the outer peripheral zone of the bit. At the same time, the channel must be positioned so that the jet emerging tangentially from the nozzle has a direction corresponding to an angle $\alpha_2 = 180°$. Under these conditions, the torque created by the outgoing fluid jet is added to the moment produced by the incoming fluid flow.

To ensure effective bottomhole cleaning under excess pressure differential conditions, as well as proper cooling of the drill bit, the torque developed by the flushing fluid discharged from the bit nozzle should be greater than the moment of the resisting forces:

$$\rho Ý Ý Ý_2 Ý_2 \cos\alpha_2 - {}_{1\,1}\cos\alpha_1) > ({}_1\tau_{dyn} + {}_2\Delta\ )_{aver} \tag{38}$$

Here, f_1 and f_2 denote the cross-sectional areas of the flushing channels at the inlet and outlet of the fluid flow, respectively.

Let us accept the following assumptions $v_1 = \frac{Q}{Nf_1}$; $v_2 = \frac{Q}{Nf_2}$ and $F_1 = F_2 = \frac{\pi D_c^2}{4}$.

After inserting the expressions for v_1 and v_2 into equation (38), the following relationship is obtained:

$$\frac{\rho Q^2}{N}\left(\frac{r_1}{f_1}\cos\alpha_1 - \frac{r_2}{f_2}\cos\alpha_2\right) > \frac{\pi D_c^2}{12}\left(\tau_{dyn} + \Delta P\right) \tag{39}$$

The dynamic pressure differential in the destruction zones is then determined according to Darcy's law, in accordance with which one may write [7, 13, 22]:

$$v_{aver.} = \frac{K_{per.}}{\eta}\cdot\frac{d\Delta P}{dz} \tag{40}$$

where $v_{aver.}$ is the average filtration velocity of the fluid in the bottomhole destruction zones; $K_{per.}$ is the integral permeability of the bottomhole; η is the filtrate viscosity coefficient; $d\Delta P/dz$ is the pressure differential gradient in the destruction zones.

According to the above, the effect of suppressive pressure manifests itself when the penetration rate exceeds the fluid filtration velocity [15, 23].

The solution of equation (40) for the case of equality between the filtration velocity and the mechanical penetration rate is of certain interest.

For the filtration depth of the fluid, we take the bottomhole deepening per one revolution of the drilling tool:

$$\frac{K_{per}}{\eta}\cdot\frac{d\Delta P}{dS} = \varphi S n = V_M \tag{41}$$

where φ is a constant coefficient ($\varphi = 2$); S is the bottomhole deepening per one revolution of the drilling tool; n is the rotational speed of the drilling tool; VM is the mechanical penetration rate.

The integral of differential equation (41) is represented as:

$$\Delta P = C + \frac{\eta}{2K_{per.}}\cdot\varphi S^2 n = C + \frac{\eta}{K_{per.}}S^2 n \tag{42}$$

where C is the integration constant, which is determined from the boundary conditions $\Delta P = \Delta P_{st} = C$ at $S = 0$; then equation (42) can finally be written as:

$$\Delta P = \Delta P_{st} = \frac{\eta}{K_{per.}}\cdot S\cdot V_M = \Delta P_{st} + \Delta P_{dyn} \tag{43}$$

Since the static part of the pressure differential is effective

only at the initial stage of the bit run, before the bit begins to contact and destroy the bottomhole rock, the actual rock-cutting process is mainly governed by the dynamic components of the pressure differential, as noted above.

Using equation (41), the destruction depth per one bit revolution is transformed into the corresponding mechanical rate of penetration. Then, by substituting the value of the dynamic pressure component into equation (39) and solving the resulting expression with respect to the mechanical penetration rate, the following relationship is obtained:

$$\frac{V_M}{V_Q} = \sqrt{\frac{3\varphi}{2N} \cdot \frac{K_{per.} \cdot \rho n}{\eta} \pi D \left(\frac{r_1 \cos\alpha_1}{f_1} - \frac{r_2 \cos\alpha_2}{f_2} \right)} \qquad (44)$$

where $V_Q = \frac{Q}{F_{bh}}$ is the specific flushing fluid flow rate; F_{bh} is the bottomhole area.

In deriving the formulas, we neglect the influence of dynamic shear stress as a small quantity compared to the excess pressure.

Taking the number of flushing channels $N = 3$, $\varphi = 2$ and considering that $n = 30\omega / \pi$, formula (44) can be represented as [2-4, 12, 13]:

$$F_M = \frac{Q}{F_{bot}} \sqrt{\frac{30 K_{per} \cdot \rho\omega}{\eta}} D \left(\frac{r_1 \cos\alpha_1}{f_1} - \frac{r_2 \cos\alpha_2}{f_2} \right) \qquad (45)$$

where ω is the rotational frequency of the drilling tool.

As can be seen from formulas (44) and (45), the drilling process under conditions of excess suppressive pressure depends on three parameters:

$$X_1 = \frac{V_M}{V_0}; \quad X_2 = \frac{K_{per}\rho\omega}{\eta}; \quad X_3 = D\left(\frac{r_1 \cos\alpha_1}{f_1} - \frac{r_2 \cos\alpha_2}{f_2} \right).$$

The first parameter, X_1, expresses the relationship between the volume rate of rock removal and the unit flow rate of the flushing fluid. This parameter directly describes the rock destruction process under the action of resisting forces. The second parameter, X_2, is defined as the ratio between the lifting forces that assist rock breakage and the viscous resistance that hinders bottomhole cleaning and the transport of drilled cuttings away from the destruction zone. Therefore, X_2 reflects the mud-cake formation tendency of the drilling fluid.

The third parameter, X_3, describes the influence of the wellbore diameter together with the hydraulic characteristics of the fluid streams entering and leaving the bit flushing channels.

The analysis of equation (45) indicates that drilling efficiency can be improved when the bit is equipped with specially designed channels that direct the fluid flow as far as possible toward the peripheral region of the jet. In this case, the inlet flow should be arranged at $\alpha_1 = 0°$, while the outlet jet should leave tangentially with respect to the bit radius at $\alpha_2 = 180°$ (fig. 6).

It is of interest that equation (45) combines both technological parameters and flushing fluid parameters, as well as design features of the rock-cutting tool flushing system. Consequently, it can be used as a basis for developing regulations when designing drilling programs. This capability, in turn, ensures high drilling performance indicators under conditions of excess pressure differential action.

Based on formula (45), using practical nomography

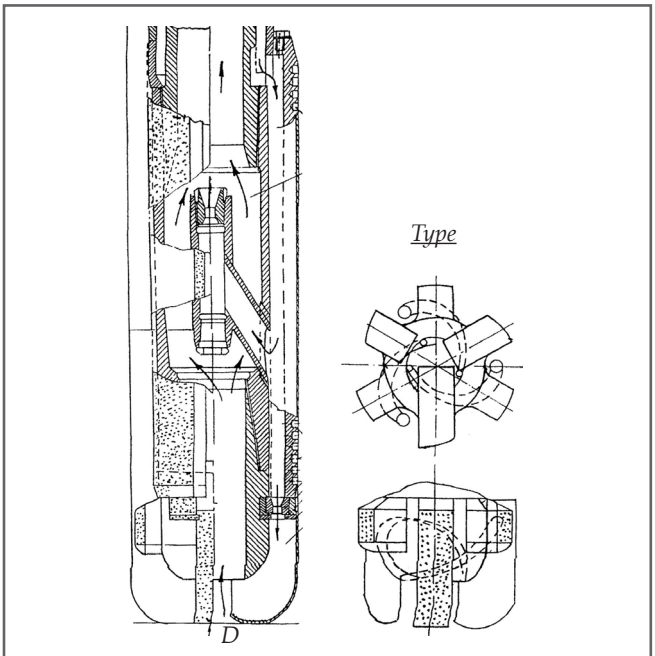

Fig. 6. Layout of the flushing system channels [1]

methods, a nomogram has been constructed for designing drilling operation parameters taking into account the character of the rocks being destroyed, the design properties of the bit flushing system, and the rheological properties of the flushing fluid (fig. 7) [11, 24].

For this reason, based on the currently used nomographic approach, a number of auxiliary intermediate parametric groups with the following structure have been proposed:

$$A = \frac{r_1 \cos\alpha_1}{f_1}; \quad A_1 = r_1 \cos\alpha_1; \quad A_2 = \frac{1}{f_2} A_1$$

$$B = \frac{r_2 \cos\alpha_2}{f_2}; \quad B_1 = r_2 \cos\alpha_1; \quad B_2 = \frac{1}{f_2} B_1$$

$$X_1 = A - B; \quad X_2 = Д \cdot X_1; \quad X_3 = \omega \cdot X_2$$

$$X_4 = \rho x_3; \quad X_5 = \frac{1}{\eta} \cdot x_4; \quad X_6 = 30 x_5 \cdot K_{пр}$$

For calculation of intermediate complexes, the following ranges of parameter variation included in (45) were used:

$$\alpha_1 = (0 \div 30)^0; \quad \alpha_2 = (90 \div 270)^0$$

$$r_1 = (10 \div 15) \cdot 10^{-3} \text{m}; \quad r_2 = (5 \div 10) \cdot 10^{-3} \text{m}$$

$$D_c = (100 \div 310) \cdot 10^{-3} \text{m}; \quad n = (500 \div 1200) \text{ rpm}$$

$$\rho = (1.2 \div 2.7) \cdot 10^3 \text{ kg/m}^3; \ \eta = (10 \div 60) \text{ Pa} \cdot \text{s}$$

$$Q = (10 \div 70) \cdot 10^{-3} \text{ m}^3/\text{s}; \ K_{per} = (100 \div 1300) \cdot 10^{-15} \text{ m}^2$$

An example of nomogram usage is given in figure 8 for parameter values equal to:

$$\alpha_1 = 15^0; \quad \alpha_2 = 150^0; \quad r_1 = 12\text{mm}; \quad r_2 = 10\text{mm}$$

$$D_c = 190 \text{ mm}; \ \omega = 120 \text{ s}^{-1}; \ \rho = 2.7 \cdot 10^3 \text{kg/m}^3; \ \eta = 20 \cdot 10^{-3} \text{ Pa} \cdot \text{s}$$

$$Q = 70 \cdot 10^{-3} \text{ m}^3/\text{s}; \ K_{per} = 1300 \cdot 10^{-15} \text{ m}^2$$

At the specified values of flushing fluid parameters, drilling modes, and drilling tool flushing system design, as shown in the nomogram, a rate of penetration (ROP) of 26.6 m/h is achieved. By changing one of the factors of either the drilling tool flushing system or the drilling mode with corresponding flushing fluid properties, a

higher value of the drilling indicator, i.e., *VM*, can be achieved [5, 23, 25, 26].

Accordingly, the method developed and illustrated by the nomogram in figure 7 makes it possible to perform a quantitative assessment of drilling efficiency in the direct formulation of the problem, while accounting for the governing process parameters. Because the underlying model incorporates variables that describe the structural features of the drilling tool, the properties of the drilling fluid, and the operating drilling regime, it also enables solution of the inverse problem – that is, selection of a mutually consistent combination of these parameters during the drilling process design stage.

In addition, the method provides a basis for evaluating the interaction mechanism between the specific energy required for rock destruction and the effectiveness of bottomhole cleaning from drilled cuttings, as reflected in the continuation of the nomogram presented in figure 7.

At the specified values of flushing fluid parameters, drilling modes, and drilling tool flushing system design, as can be seen from the nomogram, a drilling rate of 26.6 m/h will be ensured. By changing one of the factors of either the drilling tool flushing system or the drilling mode with corresponding flushing fluid properties, a higher value of the drilling indicator, i.e., *VM*, can be achieved.

Thus, the proposed approach, illustrated by the nomogram in figure 7, makes it possible to numerically assess the efficiency of the drilling process in the form of a direct problem, while taking into account the main parameters of its practical implementation. Since the original model contains variables related to the structural design of the drilling tool, the properties of the drilling fluid, and the selected drilling regime, this approach can also be used for solving the inverse problem. In other words, it enables the determination of a compatible combination of these parameters at the stage of drilling process design.

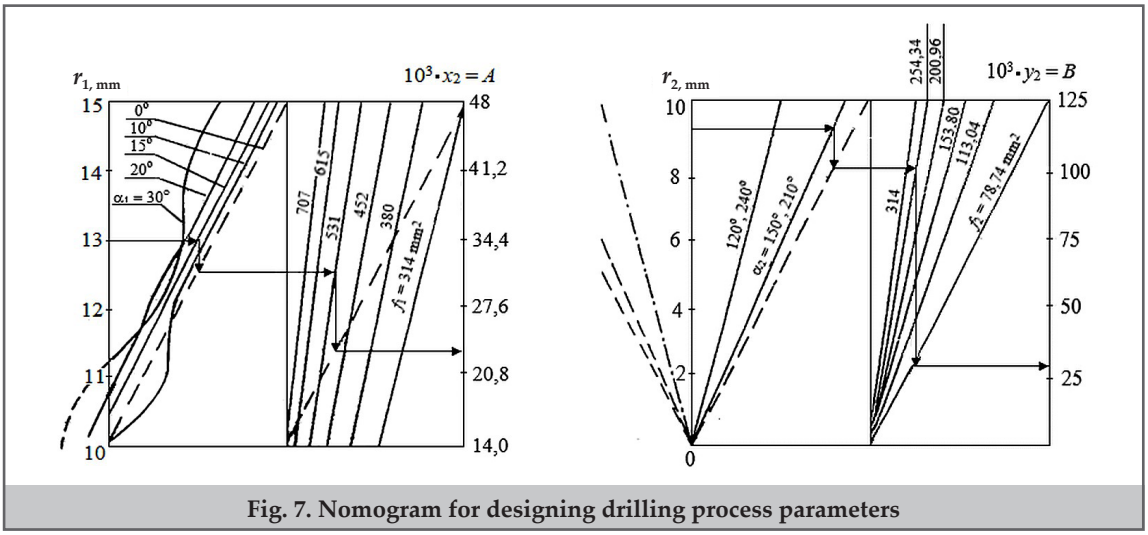

Fig. 7. Nomogram for designing drilling process parameters

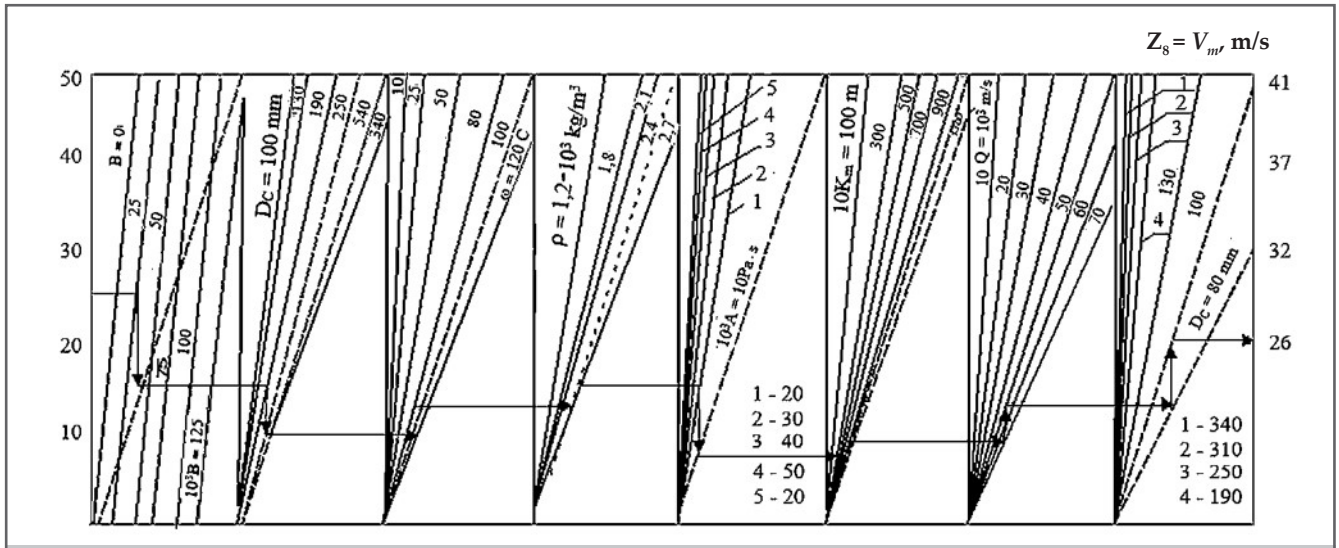

Fig. 8. Assessment of the mechanism of mutual influence between destruction specific energy consumption and quality of well bottomhole cleaning from drilled cuttings (continuation of nomogram in figure 7)

Conclusions

1. The conducted studies show that effective utilization of the hydraulic energy of the drilling mud flow can become a key factor in improving the technical and economic efficiency of drilling. This approach is of particular value when conducting operations at considerable depths, as it allows substantial reduction of energy consumption for the drilling process.

2. The requirements for the design and installation parameters of the drilling tool flushing system have

been analyzed, and their interrelation with the drilling tool operating parameters has been determined.

3. A model for optimizing the flushing system channel cross-section para-meters has been constructed, and an optimal profile ensuring the required specific energy consumption of the drilling tool has been proposed.

4. It has been determined that, under conditions of dynamic excess pressure differential, the effectiveness of drilling operations depends on a set of interrelated factors, including technological operating parameters, the properties of the flushing fluid, and the structural features of the flushing system of the rock-cutting tool.

5. A nomographic calculation and design approach has been proposed to select mutually compatible combinations of these factor groups, thereby ensuring efficient drilling performance under dynamic pressure differential conditions.

References

1. Hasanov, R. A., Mamedbekov, O. K., Medzhidov, G. N., et al. (2003). Destruction and cleaning of the bottomhole during well drilling. *Azerbaijan Republic Patent I 20030002.*

2. Hasanov, R. A., Medzhidov, G. N., Gulgazli, A. S., Medzhidov, N. A. (2002). On the kinetics of the well bottomhole cleaning process from drilled cuttings. *Oilfield Engineering*, 9, 36-38.

3. Kolesnikov, N. A., Rakhimov, A. K., Brykov, A. A., Bulatov, A. I. (1989). Rock destruction processes and reserves for increasing drilling rates. *Tashkent: Fan.*

4. Maslennikov, I. K. (1984). Improvement of drilling tools for oil wells. *Moscow: TsINTI Khimneftemash.*

5. Hu, H., Guan, Z., Zhang, B., et al. (2021). Structure design of weight-on-bit self-adjusting PDC bit based on stress field analysis and experiment evaluation. *Journal of Petroleum Science and Engineering*, 196, 107692.

6. Stoxreiter, T., Portwood, G., Gerbaud, L., et al. (2019) Full-scale experimental investigation of the performance of a jet-assisted rotary drilling system in crystalline rock. *International Journal of Rock Mechanics and Mining Sciences*, 115, 87–98.

7. Chen, P., Miska, S., Yu, M., et al. (2021). Modeling of cutting rock: from PDC cutter to PDC bit-modeling of PDC cutter. *SPE Journal*, 26(06), 3444-3464.

8. Chen, X. Y., Cao, T., Yu, K. A., et al. (2020). Numerical and experimental investigation on the depressurization capacity of a new type of jet mill bit. *Petroleum Science*, 17, 1602–1615.

9. Zhu, J., Huang, Z., Ma, Y., et al. (2020). Hydraulic structure design and downhole flow field optimization of drill bits in limestone formations. *Science Progrress*, 103(3).

10. Echt, T., Stoxreiter, T., Plank, J. (2020). Impact of drilling fluid systems on high-pressure jet-assisted rotary drilling performance. *Heliyon*, 6(6), e04179.

11. Mazen, A. Z., Mujtaba, I. M., Hassanpour, A., Rahmanian, N. (2020). Mathematical modelling of performance and wear prediction of PDC drill bits: Impact of bit profile, bit hydraulic, and rock strength. *Journal of Petroleum Science and Engineering*, 188, 106849.

12. Fang, T., Ren, F., Liu, H., et al. (2022). Progress in particle jet drilling and rock-breaking mechanisms for deep wells. *Journal of Petroleum Exploration and Production Technology*, 12, 1697–1708.

13. Khoshouei, M., Bagherpour, R. (2023). Measurement, prediction, and modeling of the drilling specific energy by soft rock properties during the drilling operation. *Measurement*, 222, 113679.

14. Wei, L., Honra, J. (2024). CFD study of multiphase bottom-hole flow fields in PDC drill bits during foam drilling. *Fluids*, 9(9), 211.

15. Al-Sudani, J. A. (2017). Real-time monitoring of mechanical specific energy and bit wear using control engineering systems. *Journal of Petroleum Science and Engineering*, 149, 171–182.

16. Vadetskiy, Yu. V. (2000). Drilling of oil and gas wells. *Moscow: Nedra.*

17. Tie, Y., Rui, X. U., Wenfeng, S., et al. (2021). Similarity evaluation of stratum anti-drilling ability and a new method of drill bit selection. *Petroleum Exploration and Development*, 48(2), 450-459.

18. Moazzeni, A. R., Khamehchi, E. (2020). Rain optimization algorithm (ROA): A new metaheuristic method for drilling opti-mization solutions. *Journal of Petroleum Science and Engineering*, 195, 107512.

19. Boukredera, F. S., Youcefi, M. R., Hadjadj, A., et al. (2023). Enhancing the drilling efficiency through the application of machine learning and optimization algorithm. *Engineering Applications of Artificial Intelligence*, 126, 107035.

20. Kalinin, A. G., Nikitin, B. A., Solodkiy, K. M., Sultanov, B. Z. (1997). Directional and horizontal well drilling: handbook. *Moscow: Nedra.*

21. Batruny, P., Zubir, H., Slagel, P., et al. (2021). Drilling in the digital age: machine learning assisted bit selection and optimization. IPTC-21299-MS. In: *The International Petroleum Technology Conference, Virtual, March.*

22. Ding, M., He, M. (2024). Effect of water-induced rock softening on rock anisotropy during drilling process. *Rock Mechanics and Rock Engineering*, 57(10), 8193-8214.

23. Elkatatny, S. (2021). Real-time prediction of rate of penetration while drilling complex lithologies using artificial intelligence techniques. *Ain Shams Engineering Journal*, 12, 917–926.

24. Dumoulin, S., Kane, A., Coudert, T., et al. (2025). Three-dimensional numerical study of DTH bit-rock interaction with HPWJ downhole slotting: Influence of bit design and bottom hole geometric conditions on rock breaking efficiency in percussive drilling. *Rock Mechanics Bulletin*, 4, 100169.

25. Seid-Rza, M. K., Faradjev, T. G., Hasanov, R. A. (1992). Prevention of complications in the kinetics of drilling processes. *Moscow: Nedra.*

26. Sugiura, J., Samuel, R., Oppelt, J., et al. (2023). Drilling modeling and simulation. *Current State and Future Goals*, 2, 143-156.